Water Resources Research

RESEARCH ARTICLE
10.1029/2020WR027644

Stable Isotope Composition of Cyclone Mekunu Rainfall, Southern Oman

Thomas Müller[1,2], Jan Friesen[3], Stephan M. Weise[3], Omar Al Abri[4], Ali Bakhit Ali Bait Said[5], and Nils Michelsen[6]

[1]Department of Hydrogeology, UFZ-Helmholtz Centre for Environmental Research, Leipzig, Germany, [2]Now at GEOMAR Helmholtz Centre for Ocean Research Kiel, Kiel, Germany, [3]Department of Catchment Hydrology, UFZ-Helmholtz Centre for Environmental Research, Halle, Germany, [4]The Research Council, Seeb, Oman, [5]Ministry of Regional Municipalities and Water Resources, Salalah, Oman, [6]Institute of Applied Geosciences, Technische Universität Darmstadt, Darmstadt, Germany

Key Points:
- We conducted high-resolution sampling of a tropical cyclone from the Arabian Sea for stable isotope and hydrochemical analyses
- The strong depletion in heavy isotopes and large intra-event variations confirm observations from tropical storms elsewhere
- There was no overlap with the isotopic fingerprint of local monsoon rains

Supporting Information:
- Supporting Information S1

Correspondence to:
T. Müller,
thmueller@geomar.de

Citation:
Müller, T., Friesen, J., Weise, S. M., Al Abri, O., Bait Said, A. B. A., & Michelsen, N. (2020). Stable isotope composition of Cyclone Mekunu rainfall, Southern Oman. *Water Resources Research*, *56*, e2020WR027644. https://doi.org/10.1029/2020WR027644

Received 4 APR 2020
Accepted 16 OCT 2020
Accepted article online 20 OCT 2020

Abstract Cyclone Mekunu hit the southern Arabian Peninsula in late May 2018 and brought rainfall amounts that accounted for up to 6 times the mean annual precipitation. Coming from the Arabian Sea, a quite underdocumented region with regard to cyclones, the storm eye crossed the Omani coast approximately 80 km east of the border to Yemen. Using automatic samplers, rainfall samples were collected during the event at three locations along a transect almost parallel to the storm track. The stable isotope analyses show a wide range of δ values, with minimum and maximum values of −17.01‰ δ^{18}O and −1.77‰ δ^{18}O and −122.2‰ δ^{2}H and −1.6‰ δ^{2}H. On average, rainfall becomes isotopically lighter with elevation, but rather irregularly. In view of high wind speeds probably precluding a gradual rainout of ascending air masses, a "pseudo elevation effect" seems likely. Our measurements expand the known δ value range of local cyclones by about 6‰ for δ^{18}O and by nearly 50‰ for δ^{2}H. The isotopic composition of the annual Indian Summer Monsoon shows values of −0.93‰ δ^{18}O to 2.21‰ δ^{18}O and −2.1‰ δ^{2}H to 23.7‰ δ^{2}H. Thus, there is a clear difference in the dual isotope signatures of the two precipitation systems in the area. Our findings enable an assessment of the impact of cyclones on the hydro(geo)logical system. For the arid Najd area, we demonstrate that the isotopic signatures of groundwater samples fall between those of cyclone and (paleo)monsoon precipitation, suggesting that several rainfall types may have contributed to replenishment.

1. Introduction

Groundwater is a crucial resource and a robust understanding of how, to what extent, and when it is replenished is important for its management (Cuthbert et al., 2019), particularly in arid regions (Abdalla & Al-Abri, 2011). Recharge occurs often disproportionately in a certain season. Depending on the study area, this could be the wet season (Jasechko et al., 2014; Lases-Hernandez et al., 2019; Matiatos & Wassenaar, 2019), the cold season (Jasechko et al., 2014, 2017), or the nongrowing season (Cherry et al., 2019). Moreover, it can occur only during specific precipitation types like intensive monthly rainfall (Jasechko & Taylor, 2015) or heavy rainfall events (Dogramaci et al., 2012; Dogramaci & Skrzypek, 2015; Li et al., 2018). Such phenomena can be studied with piezometric data (Taylor et al., 2013) and highly resolved records might reveal the effects of single storms (Abdalla & Al-Abri, 2011; Callahan et al., 2012; Dogramaci et al., 2012). Although the required long-term data sets occasionally exist (Cuthbert et al., 2019; Taylor et al., 2013), they are generally rare, especially in the tropics (Jasechko & Taylor, 2015).

The stable isotopes of water (δ^{18}O, δ^{2}H) provide a convenient alternative to this approach (Cherry et al., 2019; Jasechko et al., 2014, 2017; Jasechko & Taylor, 2015; Li et al., 2018). In such studies, the isotopic composition of groundwater is compared to the (mean) precipitation signal, and deviations are considered indicative for a predominance of recharge in a certain season or by a specific precipitation type. Importantly, this method also works in hindsight, that is, one can evaluate the groundwater's isotopic composition as an integral signal. Hence, the technique is not only applicable to modern water, but also to old groundwater and other paleoclimatic archives preserving the isotopic signature, such as speleothem calcite ($\delta^{18}O_{calcite}$) or fluid inclusions (δ^{18}O, δ^{2}H; Fleitmann & Matter, 2009, Nicholson et al., 2020).

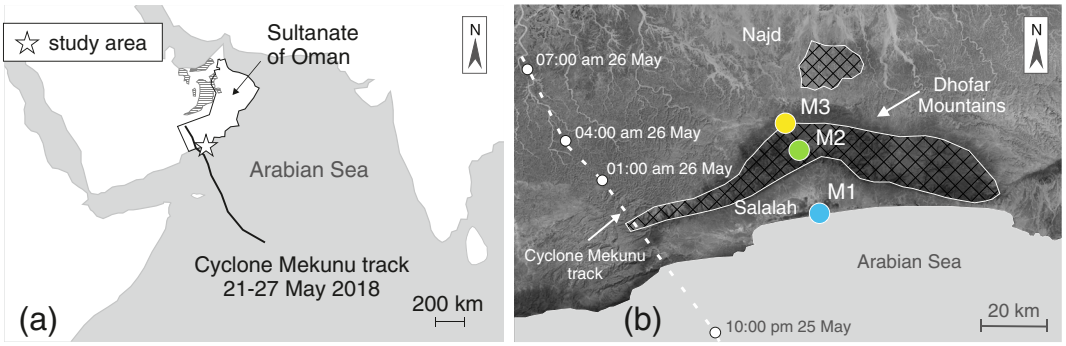

Figure 1. (a) Overview of the Cyclone Mekunu track. The cyclone originated in the Arabian Sea. First rain showers in the Sultanate of Oman occurred on 24 May. Hatched areas represent salt pans (modified from Schulz et al., 2015). (b) Sampling locations in the Salalah coastal plain and the Dhofar Mountains. Cyclone Mekunu made landfall about 45 km west of Salalah. Cross-hatched areas represent outcrops of the Umm Er Radhuma formation.

While the method is generally elegant and simple, it requires a sound knowledge of the isotopic composition of precipitation. Seasonal effects can often be evaluated with monthly long-term data from the Global Network of Isotopes in Precipitation (GNIP; IAEA/WMO, 2020). Yet, studying the relevance of extreme events, such as tropical storms (depending on the region called cyclones, hurricanes, or typhoons) for recharge is usually challenging. The main reason is that the corresponding isotope data are limited. This, in turn, is related to the often irregular and sudden occurrence of these storms, their large spatial extents, and the difficulties in predicting their course. Targeted sampling is therefore challenging. Increased attention in the scientific community, combined with unconventional approaches (e.g., public involvement in sampling) and development of sampling technology, has enabled new data for different regions, including Australia (Munksgaard et al., 2015), China (Xu et al., 2019), Costa Rica (Sánchez-Murillo et al., 2019), Japan (Fudeyasu et al., 2008; Ohsawa & Yusa, 2000), Puerto Rico (Lawrence et al., 1998), and the United States (Good et al., 2014; Lawrence et al., 1998). These studies show that storm precipitation often exhibits (1) a significant depletion in heavy isotopes and (2) large intra-event δ value variations. Yet clearly, there is still a data gap concerning tropical cyclones (Sánchez-Murillo & Durán-Quesada, 2019). The number of studies on this topic is still small, and there are regions with little or no information available. The Arabian Sea, presented here, is one of them.

The greater Salalah area in Southern Oman (Figure 1) experiences an annual monsoon (locally called *khareef*) and occasional cyclones that can deliver rainfall amounts that substantially exceed mean annual precipitation. To the best of our knowledge, the study area is the only place on the Arabian Peninsula influenced by both precipitation systems. Since the monsoon occurs every summer in the form of a quasi-continuous *drizzle* (unlike many other monsoons) and plays an important role for water supply, ecosystems and forestry, livestock grazing, and tourism (Abdul-Wahab, 2003; Friesen et al., 2018; Hildebrandt et al., 2007; Shammas, 2007), it has received considerable attention by the scientific community. Apart from seasonal precipitation amounts (typically 55 and 220 mm in the coastal plain and the Dhofar Mountains, respectively; Hildebrandt et al., 2007), also the isotopic composition of the monsoon rain has been studied. With $\delta^{18}O$ values from −0.93‰ to 2.21‰ and $\delta^{2}H$ values between 2.1‰ and 23.7‰ (daily samples; $n = 153$; Clark, 1987; Strauch et al., 2014; Wushiki, 1991), it was found to be similar to the isotopic composition of seawater. However, corresponding data on cyclones in the region are scarce and we lack an overview of possible δ value ranges and spatial heterogeneities. Whether cyclones show a classical elevation effect (depletion in heavy isotopes at greater elevation) is not known either. In part, this data scarcity is caused by the lack of a long-term isotope monitoring network in Oman (Weyhenmeyer et al., 2002) and also the irregular occurrence of the cyclones (every 2–6 years; Friesen et al., 2018) likely plays a role. For southern Oman five cyclone rainfall values have been reported so far, four for Cyclone O6-A in 1992 and one for Cyclone Keila in 2011 (Macumber et al., 1995; Strauch et al., 2014). During Cyclone O6-A, a sample was taken on the first day of the event and three samples 4 days later. While the first showed −1.45‰ $\delta^{18}O$ and 5.7‰ $\delta^{2}H$, the later samples were strongly depleted in heavy isotopes (arithmetic mean of −7.87‰ $\delta^{18}O$ and −61.5‰ $\delta^{2}H$). The sample of Cyclone Keila was

taken on the fifth day of the event and is even more depleted in heavy isotopes (−10.76‰ $\delta^{18}O$ and −73.0‰ $\delta^{2}H$). All samples were taken as grab samples (i.e., not as bulk samples integrating over the entire event or a specified time period) and corresponding rain amounts are unknown. Hence, these isolated samples do not allow to trace the isotopic development, to calculate Event Meteoric Water Lines, or to provide a precipitation-weighted mean isotopic composition. Data on cyclone-triggered surface runoff, sampled by the same authors, is similarly difficult to interpret.

In May 2018, Cyclone Mekunu hit the region and brought more than 500 mm of rain within a few days (Government of India, 2018; PACA, 2018). It caused devastating floods, 31 casualties, and damage exceeding 1.5 billion US$ (AON, 2018). However, it also offered the possibility to sequentially collect rain samples for isotope analyses along a transect from the coast to the Dhofar Mountains. Such data may help to clarify the general significance of extreme events on groundwater recharge. This is especially important for the area north of the Dhofar Mountains, the arid Najd, which is Oman's main agricultural area and experiences slow depletion of its water resources (Saber et al., 2017). While there is consensus that the groundwater, occurring at depths of up to 700 m, has been recharged under more humid paleoclimatic conditions (in the Early to Middle Holocene and Late Pleistocene), the mechanisms are still under debate. Some researchers favor the hypothesis that replenishment was mainly caused by a stronger (Indian Ocean) monsoon (Fleitmann et al., 2003; Matter et al., 2015; Rosenberg et al., 2011) that reached the interior of the Peninsula due to a northward shift of the Intertropical Convergence Zone (Burns et al., 1998, 2001). Others believe that (cyclonic) storms were the dominant source (Al-Mashaikhi et al., 2012; Clark, 1987; Clark et al., 1987). Stable isotopes have the potential to resolve this issue (Meredith et al., 2018; Sultan et al., 2008), but we need data for both rainfall types, i.e., monsoon *and* cyclone precipitation.

Since the lack of reliable data on the latter represents an important knowledge gap, our main questions are as follows: To what extent do local cyclone rains differ from monsoon precipitation isotopically? Do local cyclone rains show the classic elevation effect, that is, a heavy isotope depletion at greater elevation? Have cyclones been a major contributor to the Najd groundwater system in the past? Since the hydrochemical composition of cyclonic rain in the region is also largely unknown, we complement our unique isotope data with major ion analyses, which will be useful for future groundwater quality studies.

2. Cyclone Mekunu

Cyclone Mekunu formed over the Arabian Sea on 20 May 2018. Starting as a low-pressure area, the system evolved within the next 5 days into an event of the category "Extremely Severe Cyclonic Storm" (defined by wind speeds between 166 and 220 km h^{-1}; Government of India, 2018) with a minimum central pressure of 960 mbar. During its formation, promoted by high sea surface temperatures of 29°C to 31°C (Government of India, 2018), the system moved westward and then turned in a north-northwestern direction (translational speed of 10.4 km h^{-1}). The center of the storm crossed the Omani coast approximately 45 km west of the city of Salalah around midnight on 25/26 May. At this time, the system had a diameter of several hundred kilometers (Figure S1). Continuing north-northwestward, the system moved inland and reached the border of Oman on 27 May where it finally dissipated (Figure 1a). The track length of the cyclone was approximately 1,400 km (Government of India, 2018). Air mass back trajectory modeling (HYSPLIT; Stein et al., 2015; Rolph et al., 2017) suggests that contributing air masses largely originated from the Western Arabian Sea (Figure S2).

Weather station data indicate that rainfall occurred along the entire coast of Dhofar, which corresponds to a corridor of about 400 km. Rainfall was observed in the coastal plain and the Dhofar Mountains and also reached the Najd desert north of the mountains. In Salalah, 617 mm of rain fell between 23 and 27 May (Government of India, 2018). This is 5 to 6 times the mean annual precipitation of Salalah.

3. Methods

Three automatic rain collectors were installed in the coastal plain (Station M1) and the mountains (Stations M2 and M3), to measure precipitation amounts and gather samples (Table S1). To avoid postsampling evaporation, the devices harness the "tube-dip-in-water collector with pressure equilibration tube" principle (Gröning et al., 2012) and automatically collect samples in predefined time intervals (for details, see Michelsen et al., 2019). The rain was collected via a funnel and drained freely in the sampling device

below. The funnel diameter was 7.5 cm at Stations M1 and M3, and 14.5 cm at Station M2. At station M1, the collector was mounted on a roof (approximately 10 m above ground). At Stations M2 and M3, the funnel was installed at a height of 2 m. All collectors started sampling on 24 May at 04:00 p.m. Integral (i.e., cumulative) samples at 4-h intervals were taken until 12:00 p.m. on 27 May. For logistical reasons Interval 18 lasted 28 h until 28 May 04:00 p.m. From then until 29 May afternoon, when the collectors were removed, the samples were again collected at 4-h intervals. In total, this provided 23 intervals for sampling.

Station M1 was located directly at the shoreline and thus almost at sea level (10 m amsl). The stations in the mountains were at 510 m amsl (M2) and at 880 m amsl (M3), almost at the top of the Dhofar Mountains (Figure 1b). The transect length was 30 km in total, 21 km between M1 and M2 and 9 km between M2 and M3.

After dismantling the collectors, the HDPE-bottles were sealed with their original caps and electrical tape. None of the bottles had overflowed. On the next day, the samples were transported to Germany and measurements started 5 days later. The stable isotope composition of water ($\delta^{18}O, \delta^{2}H$) was measured by laser spectroscopy using isotopic liquid water analyzers (L2120-i by Picarro and TIWA-45EP by Los Gatos Instruments). We calibrated the analytical devices with the two extremes High ($\delta^{18}O = 2.85‰$, $\delta^{2}H = 1.8‰$) and Low ($\delta^{18}O = -40.95‰$, $\delta^{2}H = -323.0‰$) and checked quality with a control standard ($\delta^{18}O = -8.43‰$, $\delta^{2}H = -57.1‰$). These lab standards were calibrated against V-SMOW (Vienna Standard Mean Ocean Water) and V-SLAP (Vienna Standard Light Antarctic Precipitation) and were confirmed in international intercomparison tests. Data evaluation was performed with LIMS for Lasers 10.095, created by the USGS and the IAEA (Coplen & Wassenaar, 2015). The results were expressed in per mil (‰) using the conventional delta-notation relative to V-SMOW. The 1σ reproducibility is commonly better than $\pm 0.2‰$ ($\delta^{18}O$) and $\pm 0.4‰$ ($\delta^{2}H$) for both instruments.

A handheld unit was used for electrical conductivity (EC) measurements (Multi 3430 by WTW). Major ion concentrations were analyzed by ion chromatography (882 Compact IC plus by Metrohm) with a precision better than $\pm 3\%$.

4. Results and Discussion

4.1. Rainfall Distribution

During Cyclone Mekunu, rain was collected for six consecutive days at all three sampling locations (Figure 1b and Table 1).

When the first rain showers occurred on land on 24 May, the storm eye was about 330 km to the south of the Salalah coastal plain. The largest rain amount for the whole 6-day period, a total of 745 mm, was measured at station M3. At stations M1 and M2, the total amounts were much smaller, 298 and 242 mm, respectively. The highest daily amounts occurred on 25 May. The values recorded at M3 (398 mm) and M1 (171 mm) exceed the corresponding mean annual precipitation amounts (based on data from 1992–2014, see Friesen et al., 2018). From 25 May 04:00 p.m. to 26 May 04:00 a.m. (when the storm made landfall; Intervals 7, 8, and 9), 384 mm of precipitation were measured at station M3 and 117 mm at station M2. In both cases, this is about 50% of the total event precipitation. At station M1, about 125 mm were recorded in this phase, corresponding to approximately 40% of the total event rainfall. During this period, the eye of the storm was closest to the sampling stations (approximately 70 km, Figure 2).

Rainfall amounts first increased at the coastal station M1 (slightly before M2 and M3), but the maximum coincided with landfall (Interval 7; 25 May 04:00 to 08:00 p.m.). A second, much smaller peak was recorded at all stations during the night of 26/27 May (Figure 2).

At station M3, rain occurred during each interval ($n = 23$); at stations M2 ($n = 20$) and M1 ($n = 13$) there are periods with no rain (Table 1 and Figure 2). Although rainfall was observed for each interval at the highest station M3 and almost all intervals at station M2, there is no overall trend of increasing rain *amounts* with elevation. The corresponding order for the total rainfall is M3 at 880 m amsl (745 mm), M1 at 10 m amsl (298 mm), and M2 at 510 m amsl (242 mm). This is interpreted as a typical characteristic of storm events with a heterogeneous rainfall distribution (e.g., due to spiral rain bands and the less rainy areas between them; see Figure S1). These features and the general movement of the system lead to significant spatiotemporal heterogeneities of rainfall amounts, a characteristic that also has been observed in other cyclone studies (Good et al., 2014).

Table 1
Precipitation Depths and Isotopic Signatures of Samples Collected at the Stations M1, M2, and M3 During Cyclone Mekunu

		M1				M2				M3			
Interval	Date	P (mm)	δ^{18}O (‰)	δ^{2}H (‰)	d^{a} (‰)	P (mm)	δ^{18}O (‰)	δ^{2}H (‰)	d^{a} (‰)	P (mm)	δ^{18}O (‰)	δ^{2}H (‰)	d^{a} (‰)
1	24 May	0.2	—	—	—	1.6	−8.44	−57.2	10.3	5.0	−5.75	−37.8	8.2
2	24 May	1.0	—	—	—	0.9	−8.54	−65.3	3.0	3.3	—	—	—
3	24 May	2.3	—	—	—	6.0	−10.38	−77.2	5.8	17.0	−11.17	−76.5	12.9
4	25 May	8.0	−8.05	−55.5	8.9	2.7	−8.66	−62.4	6.9	18.6	−9.36	−60.9	14.0
5	25 May	35.8	−10.94	−75.8	11.7	1.2	−7.53	−54.5	5.7	6.1	−8.89	−57.8	13.3
6	25 May	18.6	−10.34	−74.0	8.7	18.3	−8.89	−64.3	6.8	25.4	−8.11	−53.5	11.4
7	25 May	97.2	−12.45	−88.3	11.3	53.0	−14.74	−106.9	11.0	181.5	−14.63	−104.3	12.7
8	25 May	9.6	−11.40	−81.1	10.1	44.0	−16.22[b]	−118.3	11.5	131.2	−17.01	−122.2	13.9
9	25 May	0.4	—	—	—	20.0	−14.39	−102.9	12.2	71.7	−16.04	−114.6	13.7
10	26 May	—	—	—	—	5.0	−7.63	−50.1	10.9	30.4	−8.93	−59.7	11.7
11	26 May	—	—	—	—	3.4	−7.27	−47.3	10.9	19.2	−8.39	−55.6	11.5
12	26 May	—	—	—	—	0.1	—	—	—	12.8	−8.03	−52.2	12.0
13	26 May	—	—	—	—	4.1	−6.64	−41.8	11.3	38.5	−8.47	−54.8	13.0
14	26 May	41.6	−8.80	−57.1	13.3	38.2	−10.97	−73.6	14.2	58.6	−11.06	−73.8	14.7
15	26 May	29.9	−7.61	−50.1	10.8	15.6	−10.28	−70.8	11.4	16.3	−11.15	−75.6	13.6
16	27 May	—	—	—	—	1.1	−8.79	−58.1	12.2	2.6	−7.93	−51.8	11.6
17	27 May	—	—	—	—	0.2	—	—	—	6.9	−9.33	−61.1	13.5
18	27 May	19.2	−5.68	−34.2	11.2	13.8	−6.24	−35.8	14.1	41.7	−5.61	−31.7	13.2
19	28 May	—	—	—	—	—	—	—	—	10.4	−2.01	−3.3	12.8
20	28 May	—	—	—	—	—	—	—	—	4.2	—	—	—
21	28 May	—	—	—	—	0.4	—	—	—	15.4	−1.77	−1.6	12.6
22	29 May	—	—	—	—	12.3	−5.47	−29.3	14.5	22.0	−5.96	−34.7	13.0
23	29 May	34.0	—[b]	—[b]	—[b]	—	—	—	—	6.1	—	—	—
weighted mean			−10.27	−70.9			−11.99	−84.5			−12.14	−84.0	

[a]Deuterium excess: $d = \delta^{2}\text{H-}8\cdot\delta^{18}\text{O}$ (Dansgaard, 1964). [b]Sample lost.

The last coordinates for the storm center are given for the morning of 27 May (Interval 15) with the center around 280 km to the northwest of the sampling stations (Government of India, 2018). Even though the low-pressure area was not classified as a cyclone anymore, rain occurred for another 3 days (Intervals 16 to 23).

4.2. Rainfall Stable Isotope Composition

Stable isotope signatures are available for 8 (M1), 17 (M2), and 20 (M3) of the 23 intervals (Table 1). The smallest number (8) also represents the number of intervals for which data are available for all three stations: Intervals 4, 5, 6, 7, 8, 14, 15, and 18 (Figure 2).

The overall minimum and maximum δ values occurred at station M3. The δ^{18}O and δ^{2}H values range from −17.01‰ to −1.77‰ and from −122.2‰ to −1.6‰, respectively (Table 1). The temporal evolution of the δ values was similar for stations M3 and M2, while the few values of station M1 allow only limited comparison (Figure 2). The most negative δ^{18}O and δ^{2}H values at all stations were observed during the rainfall peak in the night of 25/26 May: −17.01‰ and −122.2‰ at M3, −16.22‰ and −118.3‰ at M2, and −12.45‰ and −88.3‰ at M1. The second rainfall peak in the night of 26/27 May (see section 4.1) also coincides with a drop in δ values, albeit a more moderate one. The least negative δ^{18}O and δ^{2}H values were observed toward the end of the event, during Intervals 18 to 22. In this phase, the δ^{18}O and δ^{2}H values reached their maxima of −1.77‰ and −1.6‰ at M3, −5.47‰ and −29.3‰ at M2, and −5.68‰ and −34.2‰ at M1 (Table 1). The observed pattern indicates a relation between the distance to the cyclone eye, the rain amount, and its isotopic composition (Figure S3). With decreasing distance to the storm eye and thus to the associated eye walls that contain the moisture (see also Figure S1), rain amounts increase and, in turn, the isotopic composition becomes more depleted in heavy isotopes. The reverse happens with increasing distance when the storm moves away from the area.

The generally light isotopic signatures of our samples are attributable to efficient vapor condensation, which is generally promoted by the size and longevity of cyclonic events, as well as their great cloud heights (Lawrence et al., 1998; here about 15 km; Cardellach et al., 2019). Moreover, isotopic exchange between

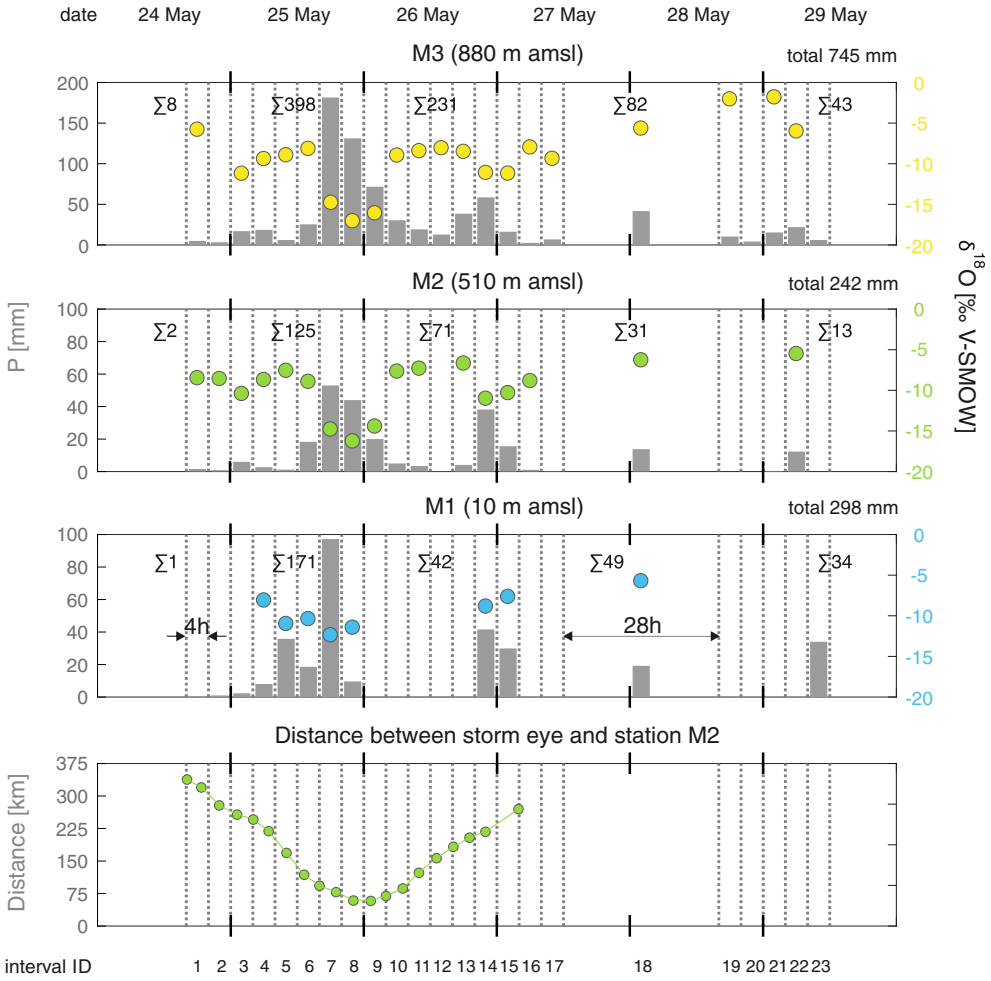

Figure 2. Sequential rain amounts and $\delta^{18}O$ signatures of Cyclone Mekunu. $\sum$ indicates the daily precipitation amount (mm). The highest amounts occurred at station M3 (note the different scale) at the top of the Dhofar Mountains, the lowest amounts were measured at station M2. The most negative $\delta^{18}O$ values coincide with greater precipitation depths and smallest distance between the storm eye and the sampling locations.

falling rain and converging vapor frequently plays a role (Lawrence et al., 1998; Munksgaard et al., 2015). The encountered periodic pattern, in turn, is associated with spiral rain bands passing our sampling locations (e.g., Munksgaard et al., 2015; see also Figure S1). The theoretical background of this trend was calculated by Lawrence and Gedzelman (1996) applying a Rayleigh-type distillation process with progressing rain bands.

In dual isotope space, our data points follow the Global Meteoric Water Line (GMWL; Craig, 1961; see Figures 3 and S4–S6), resulting in a moderate deuterium excess (d) range ($d = \delta^2H\text{-}8\ \delta^{18}O$; Dansgaard, 1964), between 8‰ and 15‰. Moreover, the data partly match the aforementioned wide δ value ranges for cyclonic storms in the region (Macumber et al., 1995; Strauch et al., 2014), but also expand the known range by about 6‰ for $\delta^{18}O$ and by nearly 50‰ for δ^2H (Figure 3). The plot also reveals that Cyclone Mekunu showed large intra-event δ value variations, confirming observations for cyclonic storms elsewhere (Gedzelman & Lawrence, 1982; Munksgaard et al., 2015). The latter authors, for instance, report $\delta^{18}O$ and δ^2H ranges of −20.2‰ to −4.8‰ and −122.2‰ to −1.6‰ for Cyclone Ita in Australia (April 2014). Even larger ranges from −21.06‰ to −1.89‰ and from −161.0‰ to 17.3‰ have been reported for the Mesoamerican and Caribbean region by Sánchez-Murillo et al. (2019).

The precipitation-weighted mean values for $\delta^{18}O$ and δ^2H are −12.14‰ and −84.0‰ for M3, −11.99‰ and −84.5‰ for M2, and −10.27‰ and −70.9‰ for M1. These values clearly reflect the influence of the negative δ values associated with the peak rainfall during the night of 25/26 May. It is also noteworthy that the

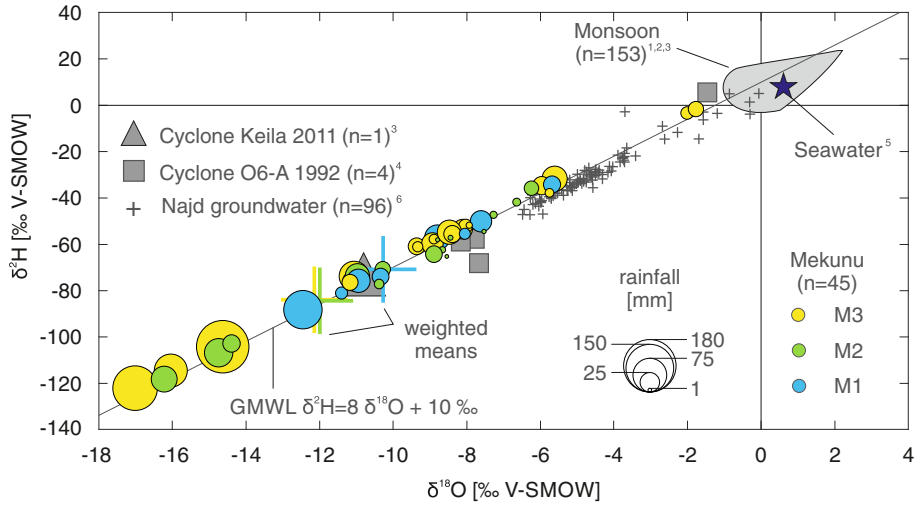

Figure 3. δ^2H-δ^{18}O relation in Cyclone Mekunu rainfall. Symbol sizes reflect the rainfall amount of the corresponding interval (mostly 4 h). For comparison literature data for monsoon (daily samples), cyclones (grab samples), and Najd groundwater are shown: 1 = Clark (1987), 2 = Wushiki (1991), 3 = Strauch et al. (2014), 4 = Macumber et al. (1995), 5 = Lambs et al. (2011), and 6 = Al-Mashaikhi (2011). Note that there is no overlap with monsoon precipitation.

weighted mean δ values become more negative with elevation, suggesting an elevation effect. On the other hand, we have to acknowledge (1) that the values for stations M2 (510 m amsl) and M3 (880 m amsl) are very similar and (2) that the prevailing wind speeds (up to 175 km h^{-1}) do probably not allow for a regular gradual rainout of air masses ascending the mountains. Hence, the effect is more likely to represent a "pseudo elevation effect."

Overall, our storm samples confirm the isotopic difference between cyclones and the annual monsoon postulated in previous studies based on a much smaller and partly erratic data set (few grab samples; Macumber et al., 1995; Strauch et al., 2014). Although a few of our samples are only slightly depleted in heavy isotopes, there is no overlap of monsoon and cyclone precipitation (Figure 3)—although both weather systems have their origin in the Arabian Sea (Figures 1a and S2).

The reason is twofold. First, the size, longevity, and cloud heights of Cyclone Mekunu cause an efficient vapor condensation, leading to an isotopically light composition (see above). Second, the annual monsoon exhibits a unique isotopic signature as well. It shows a small δ value scatter, with δ^{18}O and δ^2H values ranging from −0.93‰ to 2.21‰ and from −2.1‰ to 23.7‰, respectively (n = 153; Clark, 1987; Strauch et al., 2014; Wushiki, 1991). The reason for this small scatter and the similarity to the seawater signature (somewhat untypical for monsoon rainfall) is a relatively short atmospheric residence time and a first-stage condensation process (Clark, 1987).

4.3. Chemistry

The hydrochemical data obtained for the Cyclone Mekunu samples are presented in Tables S2–S4. The EC was highly variable, ranging between 6 and 375 µS cm^{-1}. The EC was highest for the coastal station M1 and was often associated with small precipitation amounts (Table S2 and Figure S7). The remarkable salinity range and the tendency of higher solute concentrations at station M1 (especially Na^+ and Cl^-) are also reflected in Figure 4a. Since the data points plot on or close to the seawater dilution line, it seems likely that the two ions have a sea spray origin (note wind speeds of up to 175 km h^{-1}; Government of India, 2018). Yet, not all ions are derived from sea spray. When plotting Ca^{2+} against Cl^-, for instance, the bulk of the data points lie above the seawater dilution line (Figure 4b). Hence, the samples have a higher concentration of Ca^{2+} than one would expect based on the corresponding Cl^- value and an assumed ion ratio resembling that of seawater (Ca^{2+} excess). This excess is particularly high for the inland stations M2 and M3 and suggests an additional Ca^{2+} source (apart from seawater). As SO_4^{2-} concentrations were also higher (Figure 4c; SO_4^{2-} excess), atmospheric dust rich in gypsum and/or anhydrite ($CaSO_4 \cdot 2H_2O$, $CaSO_4$) is a potential

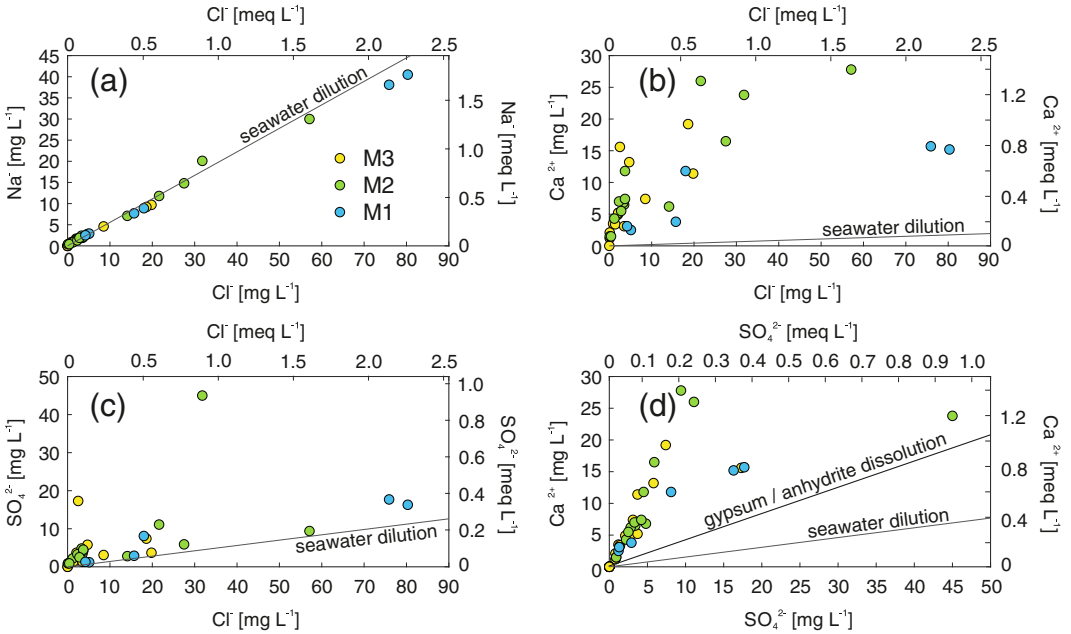

Figure 4. (a–d) Major ion scatter plots for samples of Cyclone Mekunu. Values for the construction of the seawater dilution line were taken from Appelo and Postma (2004).

source. In the study area, these minerals occur in the Eocene Rus formation cropping out north of the Dhofar Mountains (Beydoun, 1966). However, also salt pans that cover large parts of the southeastern Arabian Peninsula (approximately 36,500 km^2; Schulz et al., 2015; see Figure 1a) contain these minerals. As they are known to be eroded by wind and have been traced in precipitation of the region (Michelsen et al., 2015), they represent another potential source.

Nearly all points in the Ca^{2+} versus SO_4^{2-} plot lie above the line representing gypsum/anhydrite dust dissolution (Figure 4d). This considerable Ca^{2+} excess (over SO_4^{2-}) demonstrates that there is an additional source, most likely calcite dust ($CaCO_3$). A probable candidate in this context is the limestone-dominated Umm Er Radhuma formation (Paleocene to Eocene) with large outcrops in the area, for example, at the southern flanks of the Dhofar Mountains (Beydoun, 1966; Müller et al., 2016; see Figure 1b).

While the postulated lithogenic imprint by gypsum/anhydrite and calcite is visible in samples from all stations, the two inland stations M2 and M3 are, not surprisingly, more affected (higher excess of Ca^{2+} and SO_4^{2-}) than the coastal station M1. The latter, in turn, is more influenced by sea spray (see also Figure S9).

Interestingly, elevated EC values and ion concentrations do occur at the beginning of the cyclone event but are not limited to the first intervals (cf. Michelsen et al., 2015). Instead, they also appear later, for instance, on 26 May, directly after the first rainfall peak associated with the landfall (Figures S7 and S8). For this phase, one can assume a rather wet terrain, possibly hampering local wind erosion. Hence, the elevated concentrations at late stages of the event might indicate an influence by soluble material mobilized further away and thus a larger geochemical footprint of the cyclone.

4.4. Implications for (Paleo)groundwater Recharge

In terms of the Najd groundwaters, both precipitation systems (monsoon and cyclone) are, *in principle*, recharge candidates (Figure 3). Yet, due to the great residence times of the groundwater (often thousands or ten thousands of years; Clark, 1987; Müller et al., 2016), the ancient equivalent of the monsoon (called paleomonsoon hereafter) has to be taken into account as well. In the literature, the Early to Middle Holocene (10–6 ka BP) is frequently reported as a more humid period in Southern Arabia (Burns et al., 2001; Fleitmann et al., 2003; Fuchs & Buerkert, 2008), but also parts of the Late Pleistocene (e.g., 80–75 ka BP; Burns et al., 2001; Fleitmann et al., 2011; Rosenberg et al., 2011). Based on $\delta^{18}O$ data for Omani speleothems, Burns et al. (2001) postulate a $\delta^{18}O$ value of −4‰ for the paleomonsoon in the mentioned time periods.

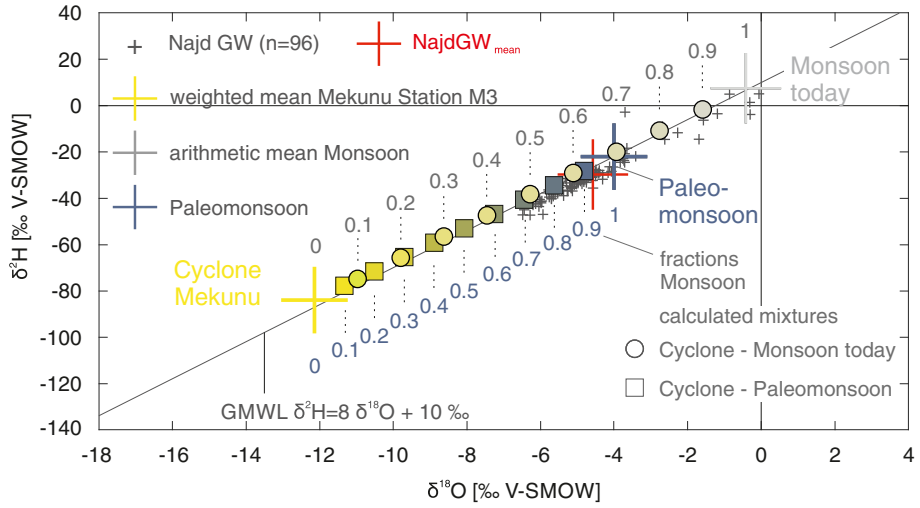

Figure 5. Results of the applied mixing model (monsoon-cyclone and paleomonsoon-cyclone). The paleomonsoon isotope signature has been derived from speleothem analyses by Burns et al. (2001).

Hence, we have to consider three isotopically distinct recharge sources for the Najd groundwater.

For cyclone recharge, we can use the precipitation-weighted means −12.14‰ δ^{18}O and −84.0‰ δ^{2}H calculated for the northernmost station M3. For today's monsoon, the arithmetic mean of 53 values from samples taken at the same location (Clark, 1987; Wushiki, 1991) is −0.42‰ δ^{18}O and 7.53‰ δ^{2}H. For the paleomonsoon, −4‰ δ^{18}O and −22‰ δ^{2}H are considered representative values.

The Najd groundwater δ^{18}O and δ^{2}H values range from −6.2‰ to −0.1‰ and from −48‰ to 5‰, respectively, and show no influence of evaporation during infiltration (Al-Mashaikhi, 2011). They plot within the isotopic signatures of all three potential recharge sources (Figure 5).

Hence, the groundwater could be a (paleo)monsoon-cyclone mix that can be described with the following mixing model.

$$\delta_{\mathrm{Mix}} = \delta_{(\mathrm{Paleo})\mathrm{monsoon}} \times f_{(\mathrm{Paleo})\mathrm{monsoon}} + \delta_{\mathrm{Cyclone}} \times f_{\mathrm{Cyclone}}, \quad (1)$$

where δ_{Mix} is the apparent mixed isotope composition, $\delta_{(\mathrm{Paleo})\mathrm{monsoon}}$ is the isotopic composition of the paleomonsoon or the monsoon, and $\delta_{\mathrm{Cyclone}}$ is the composition of the cyclone (δ^{18}O). $f_{(\mathrm{Paleo})\mathrm{monsoon}}$ and f_{Cyclone} are the corresponding recharge fractions.

If 35% cyclone recharge are mixed with 65% monsoon recharge, the resulting water matches the arithmetic mean of the Najd groundwater samples of −4.57‰ δ^{18}O and −29.73‰ δ^{2}H. The isotopically lightest groundwater signature of −6.48‰ δ^{18}O and −47.2‰ δ^{2}H, can be mimicked by choosing proportions of 52% and 48%, respectively. Although such apparent mixing ratios might seem plausible in view of Figure 3 and a recent cyclone indeed led to recharge in the Najd — Müller (2012) reports a groundwater level increase by >4 m during Cyclone Keila (November 2011), they are not appropriate for past recharge scenarios. Taking into account the long groundwater residence times, mixtures of cyclone and *paleo*monsoon waters have to be considered. In this case, significantly lower proportions of the cyclone water (7% and 30%) are required to match the isotopic composition of the groundwater (to obtain the mean and the lightest groundwater signature, respectively; Figure 5). Hence, this scenario does not require a major cyclone contribution to the recharge of the Najd groundwater.

Apart from groundwater, our findings might also be relevant for studies of high-resolution paleoclimate archives. The isotopic signature of cyclones may be recorded in freshwater mollusks (Lawrence, 1998) or tree rings (Slotta et al., 2019). Speleothems are particularly noteworthy archives on the Arabian Peninsula since much of the paleoclimatic framework is based on data from Omani caves (Burns et al., 1998, 2001; Fleitmann et al., 2003, 2004). While paleoprecipitation is commonly derived from the

$\delta^{18}O$ signature of speleothems via the amount-effect (Dansgaard, 1964), this approach might partly be oversimplified, because microphysical effects and cloud type apparently exert comparable influences on the rainfall's isotopic composition (Konecky et al., 2019). Hence, isotopic data on modern tropical cyclones may represent crucial benchmarks with the potential to improve our understanding of the underlying relations and interplays. Given the general possibility of rapid cyclone imprints on speleothems (Frappier et al., 2007) and the presence of actively growing speleothems in the study area (Fleitmann et al., 2004), it seems timely to study local speleothems to trace Cyclone Mekunu (and similar events) in this archive. This could help to understand the current impact of rain events on the underground (groundwater and speleothems) and, building on it, to draw conclusions about the occurrence and impact of storm events in the distant past.

5. Conclusions

Given that previous data on cyclone precipitation in southern Oman only comprised six values, our 45 samples from the year 2018 represent a much more solid database. They expand the known δ value range by about 6‰ for $\delta^{18}O$ and by nearly 50‰ for $\delta^{2}H$.

The strong spatiotemporal variability during the event underscores the need for sequential sampling and the calculation of precipitation-weighted means (instead of grab sampling and arithmetic means; cf. Macumber et al., 1995; Strauch et al., 2014). In principle, more stations would be helpful as well, but their number is often limited by resource constraints and safety issues.

The precipitation-weighted means decrease with elevation, but rather irregularly. Given the high wind speeds probably preventing a gradual rainout of ascending air masses, a "pseudo elevation effect" seems likely. The large number of samples in combination with rainfall amounts also allows us to calculate an overall weighted mean composition for Cyclone Mekunu (around −11‰ for $\delta^{18}O$ and −80‰ for $\delta^{2}H$).

All values from 2018 confirm more negative δ values for storm precipitation compared to monsoon rain, which is today's main precipitation source in southern Oman. Although a few samples are only slightly negative, there is no overlap between monsoon and cyclone precipitation. This observation thus also supports the results of previous cyclone studies in other areas, where little or no overlap between cyclonic storms and the background signal (usual precipitation) was observed.

Results of the hydrochemical analyses revealed that all samples were freshwater (max. EC 375 $\mu S\ cm^{-1}$) but showed variable compositions (i.e., no unique fingerprint), with a dominant sea spray impact at the coast and stronger lithogenic imprints (gypsum/anhydrite and calcite) further inland.

Our findings may be useful for a number of related fields, including hydro(geo)logy. We could for instance show that the isotopic signatures of groundwaters from the nearby Najd area fall between those of the cyclone and (paleo)monsoon rains, which suggests that several precipitation types could have contributed to recharge.

Acknowledgments

This work has been supported by the project "Submarine Groundwater Discharge: Adaption of an Autonomous Aquatic Vehicle for Robotic Measurements, Sampling and Monitoring", funded by The Research Council of Oman (TRC Research Contract No. TRC/RCP/15/001). We kindly acknowledge steady support by the Ministry of Regional Municipalities and Water Resources (MRMWR) of the Sultanate of Oman. We thank Arne Kersting and Victoria Rädle for assistance during collector installation. The authors gratefully acknowledge the NOAA Air Resources Laboratory (ARL) for the provision of the HYSPLIT transport and dispersion model used in this publication. Feedback by the editor Ilja van Meerveld as well as Steven Good and two anonymous reviewers greatly improved the manuscript.

Data Availability Statement

The precipitation stable isotope and hydrochemistry data are provided in the supporting information and are archived in the PANGAEA database (https://doi.pangaea.de/10.1594/PANGAEA.909045).

References

Abdalla, O., & Al-Abri, R. B. Y. (2011). Groundwater recharge in arid areas induced by tropical cyclones: Lessons learned from Gonu 2007 in Sultanate of Oman. *Environmental Earth Sciences*, *63*, 229–239. https://doi.org/10.1007/s12665-010-0688-y

Abdul-Wahab, S. A. (2003). Analysis of thermal inversions in the Khareef Salalah region in the Sultanate of Oman. *Journal of Geophysical Research*, *108*(D9), 4274. https://doi.org/10.1029/2002JD003083

Al-Mashaikhi, K., Oswald, S., Attinger, S., Büchel, G., Knöller, K., & Strauch, G. (2012). Evaluation of groundwater dynamics and quality in the Najd aquifers located in the Sultanate of Oman. *Environmental Earth Sciences*, *66*(4), 1195–1211. https://doi.org/10.1007/s12665-011-1331-2

Al-Mashaikhi, K. S. A. (2011). *Evaluation of groundwater recharge in Najd aquifers using hydraulics, hydrochemical and isotope evidences* (Doctoral Dissertation, Helmholtz Centre for Environmental Research, UFZ). Leipzig: UFZ.

AON (2018). *Global catastrophe recap*. London: AON. December 2018. http://thoughtleadership.aonbenfield.com/Documents/20190118-ab-if-december-global-recap.pdf (last accessed on 4 September, 2019).

Appelo, C. A. J., & Postma, D. (2004). *Geochemistry, groundwater and pollution*. Leiden, The Netherlands: A.A. Balkema Publishers.

Beydoun, Z. R. (1966). Geology of the Arabian Peninsula—Eastern Aden Protectorate and part of Dhufar. In *Geological Survey Professional Paper 560-H*. Washington, DC: USGS.

Burns, S. J., Fleitmann, D., Matter, A., Neff, U., & Mangini, A. (2001). Speleothem evidence from Oman for continental pluvial events during interglacial periods. *Geology*, *29*(7), 623–626. https://doi.org/10.1130/0091-7613(2001)029<0623:sefofc>2.0.co;2

Burns, S. J., Matter, A., Frank, N., & Mangini, A. (1998). Speleothem-based paleoclimate record from northern Oman. *Geology*, *26*, 499–502. https://doi.org/10.1130/0091-7613(2001)029<0623:sefofc>2.0.co;2

Callahan, T. J., Vulava, V. M., Passarello, M. C., & Garrett, C. G. (2012). Estimating groundwater recharge in lowland watersheds. *Hydrological Processes*, *26*, 2845–2855. https://doi.org/10.1002/hyp.8356

Cardellach, E., Oliveras, S., Rius, A., Tomás, S., Ao, C. O., Franklin, G. W., et al. (2019). Sensing heavy precipitation with GNSS polarimetric radio occultations. *Geophysical Research Letters*, *46*, 1024–1031. https://doi.org/10.1029/2018GL080412

Cherry, M., Gilmore, T., Mittelstet, A., Gastmans, D., Santos, V., & Gates, J. (2019). Recharge seasonality based on stable isotopes: Nongrowing season Bias altered by irrigation in Nebraska. *Hydrological Processes*, *34*, 1575–1586. https://doi.org/10.1002/hyp.13683

Clark, I. D. (1987). *Groundwater resources in the Sultanate of Oman: Origin, circulation time, recharge processes and paleoclimatology* (Doctoral thesis). Paris: Universite de Paris-Sud.

Clark, I. D., Fritz, P., Quinn, O. P., Rippon, P. W., Nash, H., & Al Said, S. B. B. G. (1987). Modern and fossil groundwater in an arid environment: A look at the hydrogeology of southern Oman. In *Proc. Symp. on Isotope Techniques in Water Resources Development. IAEA (Int. at. Energy Agency)* (pp. 167–187). Vienna: IAEA.

Coplen, T. B., & Wassenaar, L. (2015). LIMS for Lasers 2015 for achieving long-term accuracy and precision of δ^2H, δ^{17}O, and δ^{18}O of waters using laser absorption spectrometry. *Rapid Communications in Mass Spectrometry*, *29*, 2122–2130. https://doi.org/10.1002/rcm.7372

Craig, H. (1961). Isotopic variations in meteoric waters. *Science*, *133*, 1702–1703. https://doi.org/10.1126/science.133.3465.1702

Cuthbert, M. O., Taylor, R. G., Favreau, G., Todd, M. C., Shamsudduha, M., Villholth, K. G., et al. (2019). Observed controls on resilience of groundwater to climate variability in sub-Saharan Africa. *Nature*, *572*, 230–234. https://doi.org/10.1038/s41586-019-1441-7

Dansgaard, W. (1964). Stable isotopes in precipitation. *Tellus*, *16*(4), 436–468. https://doi.org/10.3402/tellusa.v16i4.8993

Dogramaci, S., & Skrzypek, G. (2015). Unravelling sources of solutes in groundwater of an ancient landscape in NW Australia using stable Sr, H and O isotopes. *Chemical Geology*, *393–394*, 67–78. https://doi.org/10.1016/j.chemgeo.2014.11.021

Dogramaci, S., Skrzypek, G., Dodson, W., & Grierson, P. F. (2012). Stable isotope and hydrochemical evolution of groundwater in the semi-arid Hamersley Basin of subtropical northwest Australia. *Journal of Hydrology*, *475*, 281–293. https://doi.org/10.1016/j.jhydrol.2012.10.004

Fleitmann, D., Burns, S. J., Neff, U., Mangini, A., & Matter, A. (2003). Changing moisture sources over the last 330,000 years in Northern Oman from fluid-inclusion evidence in speleothems. *Quaternary Research*, *60*, 223–232. https://doi.org/10.1016/s0033-5894(03)00086-3

Fleitmann, D., Burns, S. J., Neff, U., Mudelsee, M., Mangini, A., & Matter, A. (2004). Palaeoclimatic interpretation of high-resolution oxygen isotope profiles derived from annually laminated speleothems from Southern Oman. *Quaternary Science Reviews*, *23*(7–8), 935–945. https://doi.org/10.1016/j.quascirev.2003.06.019

Fleitmann, D., Burns, S. J., Pekala, M., Mangini, A., Al-Subbary, A., Al-Aowah, M., et al. (2011). Holocene and Pleistocene pluvial periods in Yemen, southern Arabia. *Quaternary Science Reviews*, *30*, 783–787. https://doi.org/10.1016/j.quascirev.2011.01.004

Fleitmann, D., & Matter, A. (2009). The speleothem record of climate variability in Southern Arabia. *Comptes Rendus Geoscience*, *341*(8–9), 633–642. https://doi.org/10.1016/j.crte.2009.01.006

Frappier, A. B., Sahagian, D., Carpenter, S. J., González, L. A., & Frappier, B. R. (2007). Stalagmite stable isotope record of recent tropical cyclone events. *Geology*, *35*, 111–114. https://doi.org/10.1130/g23145a.1

Friesen, J., Zink, M., Bawain, A., & Müller, T. (2018). Hydrometeorology of the Dhofar cloud forest and its implications for groundwater recharge. *Journal of Hydrology: Regional Studies*, *16*, 54–66. https://doi.org/10.1016/j.ejrh.2018.03.002

Fuchs, M., & Buerkert, A. (2008). A 20 ka sediment record from the Hajar Mountain range in N-Oman, and its implication for detecting arid–humid periods on the southeastern Arabian Peninsula. *Earth and Planetary Science Letters*, *265*(3), 546–558. https://doi.org/10.1016/j.epsl.2007.10.050

Fudeyasu, H., Ichiyanagi, K., Sugimoto, A., Yoshimura, K., Ueta, A., Yamanaka, M. D., & Ozawa, K. (2008). Isotope ratios of precipitation and water vapor observed in Typhoon Shanshan. *Journal of Geophysical Research*, *113*, D12113. https://doi.org/10.1029/2007JD009313

Gedzelman, S. D., & Lawrence, J. R. (1982). The isotopic composition of cyclonic precipitation. *Journal of Applied Meteorology*, *21*(10), 1385–1404. https://doi.org/10.1175/1520-0450(1982)021<1385:ticocp>2.0.co;2

Good, S., Mallia, D. V., Lin, J. C., & Bowen, G. J. (2014). Stable isotope analysis of precipitation samples obtained via crowdsourcing reveals the spatiotemporal evolution of Superstorm Sandy. *PLoS ONE*, *9*(3), e91117. https://doi.org/10.1371/journal.pone.0091117

Government of India, Ministry of Earth Sciences, India Meteorological Department (2018). *Extremely severe cyclonic storm, "MEKUNU" over the Arabian Sea (21–27 May 2018): A report*. New Delhi: India Meteorological Department. Retrieved from http://www.rsmcnew-delhi.imd.gov.in/index.php?option=com_content&view=article&id=198:preliminary-report-2018&catid=12:publications&Itemid=540&lang=en

Gröning, M., Lutz, H. O., Roller-Lutz, Z., Kralik, M., Gourcy, L., & Pöltenstein, L. (2012). A simple rain collector preventing water re-evaporation dedicated for δ^{18}O and δ^2H analysis of cumulative precipitation samples. *Journal of Hydrology*, *448–449*, 195–200. https://doi.org/10.1016/j.jhydrol.2012.04.041

Hildebrandt, A., Al Aufi, M., Amerjeed, M., Shammas, M., & Eltahir, E. A. B. (2007). Ecohydrology of a seasonal cloud forest in Dhofar: 1 field experiment. *Water Resources Research*, *43*, W10411. https://doi.org/10.1029/2006wr005261

IAEA/WMO–International Atomic Energy Agency/World Meteorological Organization (2020). *Global network of isotopes in precipitation*. Vienna: IAEA. Retrieved from http://www.iaea.org/water (last accessed on 24 February, 2020).

Jasechko, S., Birks, S. J., Gleeson, T., Wada, Y., Fawcett, P. J., Sharp, Z. D., et al. (2014). The pronounced seasonality of global groundwater recharge. *Water Resources Research*, *50*, 8845–8867. https://doi.org/10.1002/2014wr015809

Jasechko, S., & Taylor, R. G. (2015). Intensive rainfall recharges tropical groundwaters. *Environmental Research Letters*, *10*, 124,015. https://doi.org/10.1088/1748-9326/10/12/124015

Jasechko, S., Wassenaar, L. I., & Mayer, B. (2017). Isotopic evidence for widespread cold-season-biased groundwater recharge and young streamflow across central Canada. *Hydrological Processes*, *31*, 2196–2209. https://doi.org/10.1002/hyp.11175

Konecky, B. L., Noone, D. C., & Cobb, K. M. (2019). The influence of competing hydroclimate processes on stable isotope ratios in tropical rainfall. *Geophysical Research Letters*, *46*, 1622–1633. https://doi.org/10.1029/2018GL080188

Lambs, L., Gurumurthy, G. P., & Balakrishna, K. (2011). Tracing the sources of water using stable isotopes: First results along the Mangalore–Udupi region, south-west coast of India. *Rapid Communications in Mass Spectrometry*, *25*(19), 2769–2776. https://doi.org/10.1002/rcm.5104

Lases-Hernandez, F., Medina-Elizalde, M., Burns, S., & DeCesare, M. (2019). Long-term monitoring of drip water and groundwater stable isotopic variability in the Yucatan Peninsula: Implications for recharge and speleothem rainfall reconstruction. *Geochimica et Cosmochimica Acta*, *246*, 41–59. https://doi.org/10.1016/j.gca.2018.11.028

Lawrence, J. R. (1998). Isotopic spikes from tropical cyclones in surface waters: Opportunities in hydrology and paleoclimatology. *Chemical Geology*, *144*, 153–160. https://doi.org/10.1016/s0009-2541(97)00090-9

Lawrence, J. R., & Gedzelman, S. D. (1996). Low stable isotope ratios of tropical cyclone rains. *Geophysical Research Letters*, *23*(5), 527–530. https://doi.org/10.1029/96gl00425

Lawrence, J. R., Gedzelman, S. D., Zhang, X., & Arnold, R. (1998). Stable isotope ratios of rain and vapor in 1995 hurricanes. *Journal of Geophysical Research*, *103*(D10), 11,381–11,400. https://doi.org/10.1029/97JD03627

Li, J., Pang, Z., Kong, Y., Wang, S., Bai, G., Zhao, H., et al. (2018). Groundwater isotopes biased toward heavy rainfall events and implications on the local meteoric water line. *Journal of Geophysical Research: Atmospheres*, *123*, 6259–6266. https://doi.org/10.1029/2018JD028413

Macumber, P. G., Barghash, B. G. S., Kew, G. A., & Tennakoon, T. B. (1995). *Hydrogeologic implications of a cyclonic rainfall event in central Oman* (pp. 87–97). London: Groundwater quality. Chapman and Hall.

Matiatos, I., & Wassenaar, L. I. (2019). Stable isotope patterns reveal widespread rainy-period-biased recharge in phreatic aquifers across Greece. *Journal of Hydrology*, *568*, 1081–1092. https://doi.org/10.1016/j.jhydrol.2018.11.053

Matter, A., Neubert, E., Preusser, F., Rosenberg, T., & Al-Wagdani, K. (2015). Palaeo-environmental implications derived from lake and sabkha deposits of the southern Rub' al-Khali, Saudi Arabia and Oman. *Quaternary International*, *382*, 120–131. https://doi.org/10.1016/j.quaint.2014.12.029

Meredith, K. T., Han, L. F., Cendón, D. I., Crawford, J., Hankin, S., Peterson, M., & Hollins, S. E. (2018). Evolution of dissolved inorganic carbon in groundwater recharged by cyclones and groundwater age estimations using the ^{14}C statistical approach. *Geochimica et Cosmochimica Acta*, *220*, 483–498. https://doi.org/10.1016/j.gca.2017.09.011

Michelsen, N., Laube, G., Friesen, J., Weise, S. M., Bait Said, A. B. A., & Müller, T. (2019). Technical note: A microcontroller-based automatic rain sampler for stable isotope studies. *Hydrology and Earth System Sciences*, *23*(6), 2637–2645. https://doi.org/10.5194/hess-23-2637-2019

Michelsen, N., Reshid, M., Siebert, C., Schulz, S., Knöller, K., Weise, S. M., et al. (2015). Isotopic and chemical composition of precipitation in Riyadh, Saudi Arabia. *Chemical Geology*, *413*, 51–62. https://doi.org/10.1016/j.chemgeo.2015.08.001

Müller, T. (2012). Recharge and residence times in an arid area aquifer (Doctoral thesis). Dresden: Technische Universität Dresden.

Müller, T., Osenbrück, K., Strauch, G., Pavetich, S., Al-Mashaikhi, K.-S., Herb, C., et al. (2016). Use of multiple age tracers to estimate groundwater residence times and long-term recharge rates in arid southern Oman. *Applied Geochemistry*, *74*, 67–83. https://doi.org/10.1016/j.apgeochem.2016.08.012

Munksgaard, N. C., Zwart, C., Kurita, N., Bass, A., Nott, J., & Bird, M. I. (2015). Stable isotope anatomy of tropical cyclone Ita, North-Eastern Australia, April 2014. *PLoS ONE*, *10*(3), e0119728. https://doi.org/10.1371/journal.pone.0119728

Nicholson, S. L., Pike, A. W. G., Hosfield, R., Roberts, N., Sahy, D., Woodhead, J., et al. (2020). Pluvial periods in Southern Arabia over the last 1.1 million-years. *Quaternary Science Reviews*, *229*, 106112. https://doi.org/10.1016/j.quascirev.2019.106112

Ohsawa, S., & Yusa, Y. (2000). Isotopic characteristics of typhonic rainwater: Typhoons no. 13 (1993) and no. 6 (1996). *Limnology*, *1*(2), 143–149. https://doi.org/10.1007/s102010070021

PACA (2018). National report to panel on tropical cyclones in the bay of Bengal and Arabian Sea. In *Government of Sultanate of Oman, Public Authority of Civil Aviation. 45th Session, Muscat, Sultanate of Oman 23–27 Sep 2018*. Muscat: Directorate General of Meteorology.

Rolph, G., Stein, A., & Stunder, B. (2017). Real-time Environmental Applications and Display sYstem: READY. *Environmental Modelling & Software*, *95*, 210–228. https://doi.org/10.1016/j.envsoft.2017.06.025

Rosenberg, T. M., Preusser, F., Fleitmann, D., Schwalb, A., Penkman, K., Schmid, T. W., et al. (2011). Humid periods in southern Arabia: Windows of opportunity for modern human dispersal. *Geology*, *39*(12), 1115–1118. https://doi.org/10.1130/g32281.1

Saber, M., Alhinai, S., Al Barwani, A., AL-Saidi, A., Kantoush, S. A., Habib, E., & Borrok, D. M. (2017). Satellite-based estimates of groundwater storage changes at the Najd aquifers in Oman. In O. Abdalla, A. Kacimov, M. Chen, A. Al-Maktoumi, T. Al-Hosni, I. Clark (Eds.), *Water resources in arid areas: The way forward* (pp. 155–169). Basel: Springer.

Sánchez-Murillo, R., & Durán-Quesada, A. M. (2019). Preface to stable isotopes in hydrological studies in the tropics: Ecohydrological perspectives in a changing climate. *Hydrological Processes*, *33*, 2160–2165. https://doi.org/10.1002/hyp.13305

Sánchez-Murillo, R., Durán-Quesada, A. M., Esquivel-Hernández, G., Rojas-Cantillano, D., Birkel, C., Welsh, K., et al. (2019). Deciphering key processes controlling rainfall isotopic variability during extreme tropical cyclones. *Nature Communications*, *10*, 4321. https://doi.org/10.1038/s41467-019-12062-3

Schulz, S., Horovitz, M., Rausch, R., Michelsen, N., Mallast, U., Köhne, M., et al. (2015). Groundwater evaporation from salt pans: Examples from the eastern Arabian Peninsula. *Journal of Hydrology*, *531*, 792–801. https://doi.org/10.1016/j.jhydrol.2015.10.048

Shammas, M. I. (2007). Impact of the Al-Qara mountain fogwater forest on groundwater recharge in the Salalah coastal aquifer, Sultanate of Oman. *Ecohydrology & Hydrobiology*, *7*(1), 37–49. https://doi.org/10.1016/s1642-3593(07)70187-8

Slotta, F., Wacker, L., Riedel, F., Heußner, K.-U., Hartmann, K., & Helle, G. (2019). High resolution ^{14}C bomb-peak dating and climate response analyses of subseasonal stable isotope signals in wood of the African baobab—A case study from Oman. *Biogeosciences Discussions*. https://doi.org/10.5194/bg-2019-325

Stein, A. F., Draxler, R. R., Rolph, G. D., Stunder, B. J. B., Cohen, M. D., & Ngan, F. (2015). NOAA's HYSPLIT atmospheric transport and dispersion modeling system. *Bulletin of the American Meteorological Society*, *96*, 2059–2077. https://doi.org/10.1175/bams-d-14-00110.1

Strauch, G., Al-Mashaikhi, K. S., Bawain, A., Knöller, K., Friesen, J., & Müller, T. (2014). Stable H and O isotope variations reveal sources of recharge in Dhofar, Sultanate of Oman. *Isotopes in Environmental and Health Studies*, *50*(4), 475–490. https://doi.org/10.1080/10256016.2014.961451

Sultan, M., Sturchio, N., Al Sefry, S., Milewski, A., Becker, R., Nasr, I., & Sagintayev, Z. (2008). Geochemical, isotopic, and remote sensing constraints on the origin and evolution of the Rub Al Khali aquifer system, Arabian Peninsula. *Journal of Hydrology*, *356*, 70–83. https://doi.org/10.1016/j.jhydrol.2008.04.001

Taylor, R. G., Todd, M. C., Kongola, L., Maurice, L., Nahozya, E., Sanga, H., & MacDonald, A. M. (2013). Evidence of the dependence of groundwater resources on extreme rainfall in East Africa. *Nature Climate Change*, *3*, 374–378. https://doi.org/10.1038/nclimate1731

Weyhenmeyer, C. E., Burns, S. J., & Waber, H. N. (2002). Isotope study of moisture sources, recharge areas, and groundwater flow paths within the eastern Batinah coastal plain, Sultanate of Oman. *Water Resources Research*, *38*(10), 1184. https://doi.org/10.1029/2000wr000149

Wushiki, H. (1991). $^{18}O/^{16}O$ and D/H of the meteoric waters in South Arabia. *Journal of the Mass Spectrometry Society of Japan*, *39*(5), 239–250. https://doi.org/10.5702/massspec.39.239

Xu, T., Sun, X., Hong, H., Wang, X., Cui, M., Lei, G., et al. (2019). Stable isotope ratios of typhoon rains in Fuzhou, Southeast China, during 2013–2017. *Journal of Hydrology*, *570*, 445–453. https://doi.org/10.1016/j.jhydrol.2019.01.017

References From the Supporting Information

CIMSS (2018). *CIMSS satellite blog. Cooperative Institute for Meteorological Satellite Studies, University of Wisconsin—Madison*. USA, Madison: University of Wisconsin-Madison. Retrieved from https://cimss.ssec.wisc.edu/satellite-blog/archives/28127 (last accessed on 5 September, 2020).

Crawford, J., Hughes, C. E., & Lykoudis, S. (2014). Alternative least squares methods for determining the meteoric water line, demonstrated using GNIP data. *Journal of Hydrology*, *519*, 2331–2340. https://doi.org/10.1016/j.jhydrol.2014.10.033